Supporting Information

Isomer Engineering for Deep Understanding Aggregation-induced Photothermal Enhancement in Conjugated System

Peiyang Gu*, Tengfei He,* Zuoyu Wang, Shifan Wang, Liming Dong, Hanning Yao, Tao Jia,* Guankui Long, Guangfeng Liu, Hua Sun*

Experimental

1. Materials

All reagents and chemicals were purchased from commercial sources and used without further purification unless stated otherwise. 2,7-dibromobenzo[1,2-*b*:4,3-*b'*]dithiophene-4,5-dione and 2,7-dibromobenzo[2,1-*b*:3,4-*b'*]dithiophene-4,5-dione were purchased from SunaTech Inc (Suzhou). 4-methoxy-*N*-(4-methoxyphenyl)-*N*-(4-(4,4,5,5-tetramethyl-1,3,2-dioxaborolan-2-yl)phenyl)aniline,[1] TBP-2Br[2] and *i*-TBP-2Br[3] were synthesized according to literature procedures.

2. Characterization

^{1}H and ^{13}C NMR spectra were collected on a Bruker 400 MHz and 101 MHz spectrometer. Mass spectra analysis was performed on TOF-MS (Waters Q-TOF). The simulations were performed by density functional theory (DFT) using the B3LYP hybrid function with the basis set 6-31G(d). Quantum chemical calculation was performed with the Gaussian 16 package.[4] The recombination energy and Huang-Rhys (H-R) factor were performed on the MOMAP program with toluene environment. Solution and thin-film UV-vis absorption spectra were recorded on a PerkinElmer Lambda 750 UV-vis spectrophotometer. The photoluminescence (PL) spectra were recorded on a F4700 spectrometer (Hitachi). Grazing-incidence wide-angle X-ray scattering (GIWAXS) measurements were carried out on a Xeuss 3.0 SAXS/WAXS system (Xenocs SA, France). The samples were prepared on Si substrates. Femtosecond transient absorption measurements were performed using a femtosecond transient absorption spectrometer system (Harpia, Lithuania). The excitation wavelength was

350 nm, with a pump power of 1 μJ cm^{-2}. The femtosecond laser source used was a PHAROS model with a repetition frequency of 89 kHz and a pulse width of approximately 150 fs (-10 ps to 8 ns). The detector speed was set to 89 kHz.
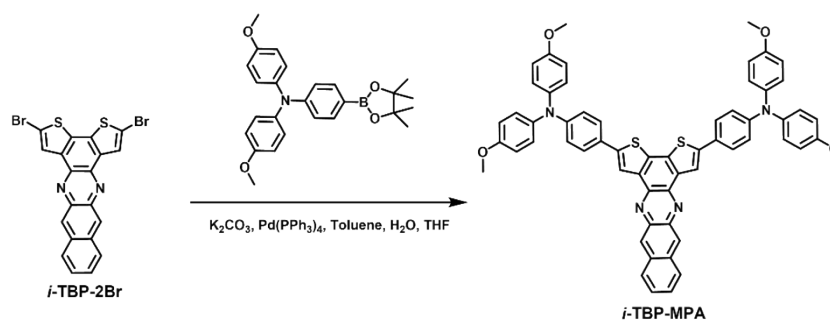
3. Synthesis of TBP-MPA
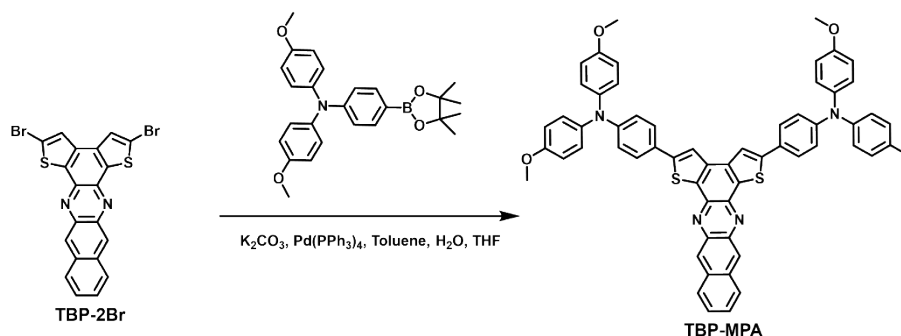
Scheme S1. Synthetic route to TBP-MPA.

The synthetic route to TBP-MPA is shown in Scheme S1, and the details of synthetic procedures are according to the literature report.[2] Under a nitrogen atmosphere, a mixture of TBP-2Br (300 mg, 0.60 mmol), 4-methoxy-*N*-(4-methoxyphenyl)-*N*-(4-(4,4,5,5-tetramethyl-1,3,2-dioxaborolan-2-yl)phenyl)aniline (570 mg, 1.32 mmol), Pd(PPh$_3$)$_4$ (27 mg, 0.02 mmol) and K$_2$CO$_3$ (2.76 g, 0.02 mol) in a solution of H$_2$O (10 mL), toluene (20 mL) and THF (20 mL) was stirred and heated at 80 °C for 15 h. When the reaction was completed, the mixture was extracted with DCM for two times. The combined organic solution was washed with sodium chloride solution and dried by anhydrous sodium sulfate. After removal of the solvent, the residue was purified by flash column chromatography (silica gel, dichloromethane/hexane = 1:1). To further purify the obtained product, we dissolved it in dichloromethane and then added a small amount of methanol to the upper layer. After evaporation, we obtained a black TBP-MPA powder with a yield of 80% (455 mg). ^{1}H NMR (400 MHz, CDCl$_3$) δ (ppm) 8.81 (s, 2H), 8.11-8.09 (m, 2H), 7.72 (s, 2H), 7.63 (d, *J* = 8.4 Hz, 4H), 7.53-7.50 (m, 2H), 7.14 (d, *J* = 8.8 Hz, 8H), 6.98 (d, *J* = 8.8 Hz, 4H), 6.90 (d, *J* = 8.8 Hz, 8H), 3.83 (s, 12H). ^{13}C NMR (101 MHz, CDCl$_3$) δ 156.49, 156.34, 149.94, 149.32, 140.89, 140.21, 140.05, 138.52, 137.95, 133.63, 132.85, 130.38, 128.39, 127.45, 127.11, 127.01, 126.72, 126.22, 125.46, 119.71, 117.15, 114.85, 55.53. MS (TOF-MS, m/z): Calcd. for C$_{60}$H$_{44}$N$_4$O$_4$S$_2$: 948.2804; found, 949.2888 [M+1].

4. Synthesis of *i*-TBP-MPA

Scheme S2. Synthetic route to *i*-TBP-MPA.

The synthetic route to *i*-TBP-MPA is shown in Scheme S2, and the details of synthetic procedures are according to TBP-MPA. ^{1}H NMR (400 MHz, CDCl$_3$) δ (ppm) 8.74 (s, 2H), 8.27 (s, 2H), 8.06-8.04 (m, 2H), 7.54 (d, *J* = 8.8 Hz, 4H), 7.49-7.47 (m, 2H), 7.13 (d, *J* = 8.4 Hz, 8H), 6.96 (d, *J* = 8.4 Hz, 4H), 6.89 (d, *J* = 8.8 Hz, 8H), 3.83 (s, 12H). ^{13}C NMR (101 MHz, CDCl$_3$) δ 156.19, 148.76, 143.23, 140.88, 140.42, 138.30, 135.33, 134.36, 133.70, 128.40, 127.13, 126.96, 126.76, 126.23, 125.53, 120.01, 118.66, 114.82, 55.53. MS (TOF-MS, m/z): Calcd. for C$_{60}$H$_{44}$N$_4$O$_4$S$_2$: 948.2804; found, 949.2881 [M+1].
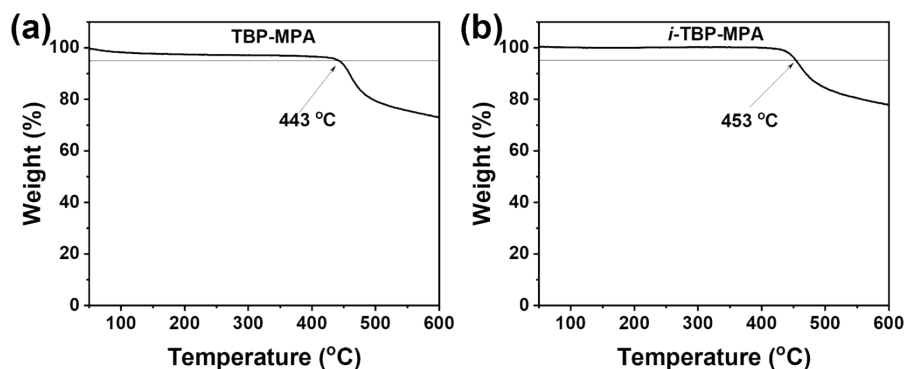

Figure S1. TGA curves of (a) TBP-MPA and (b) *i*-TBP-MPA (heating rate: 10 °C min^{-1}, N$_2$ atmosphere).
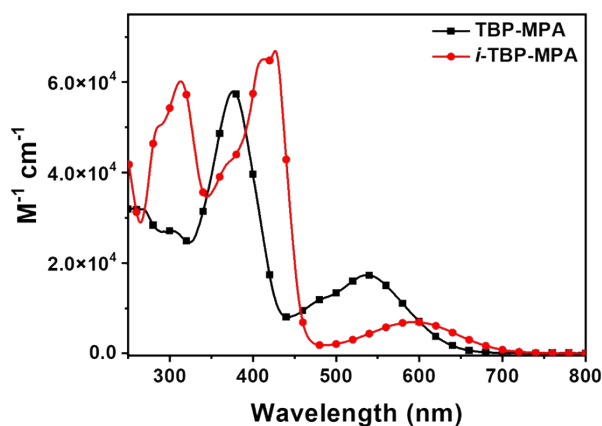

Figure S2. Absorption coefficient spectra of TBP-MPA and *i*-TBP-MPA in chloroform.
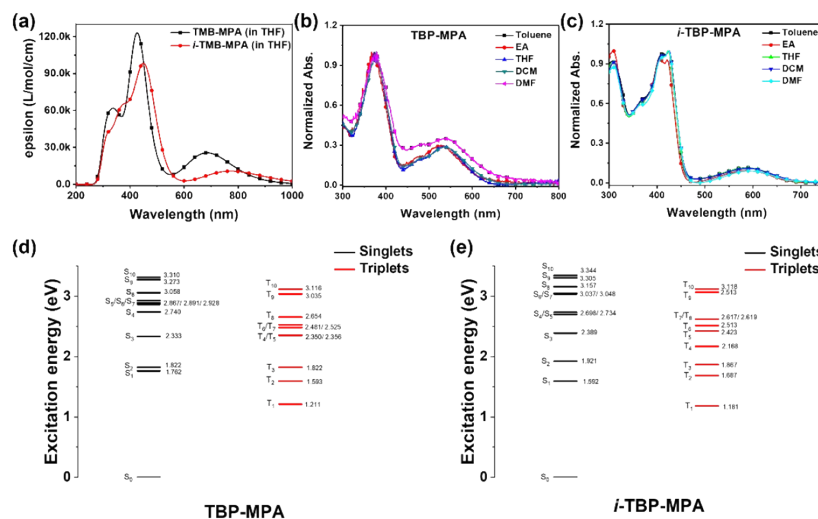
Figure S3. (a) Theoretical UV-visible absorption spectra of TBP-MPA and *i*-TBP-MPA in THF solution. Normalized UV-vis absorption spectra of (b) TBP-MPA and (c) *i*-TBP-MPA in solvents of various polarities. (d) DFT calculated energy level diagrams of TBP-MPA and *i*-TBP-MPA.
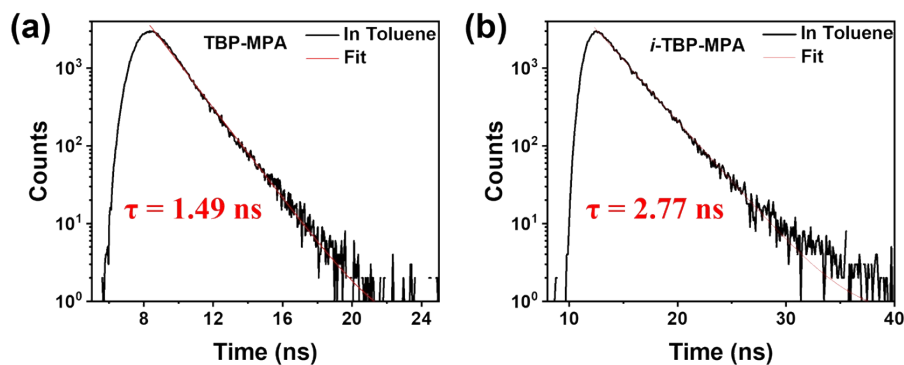

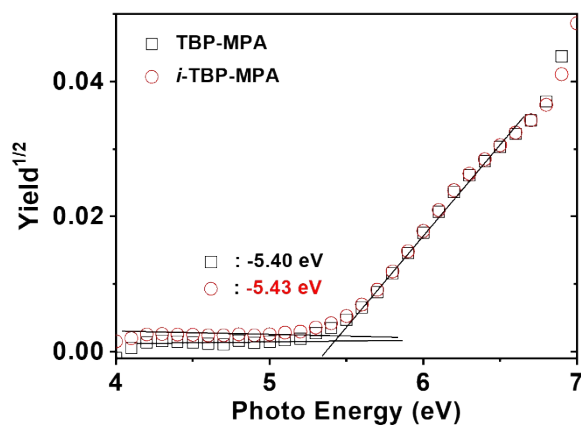**Figure S4.** Transient PL decay of (a) TBP-MPA and (b) *i*-TBP-MPA in Toluene.

Figure S5. HOMO energy levels of TBP-MPA and *i*-TBP-MPA as measured by photoelectron yield spectroscopy.
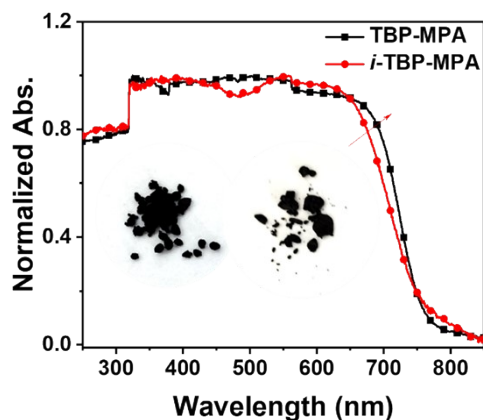
Figure S6. Absorption spectra of TBP-MPA and *i*-TBP-MPA solid powder with inset images.
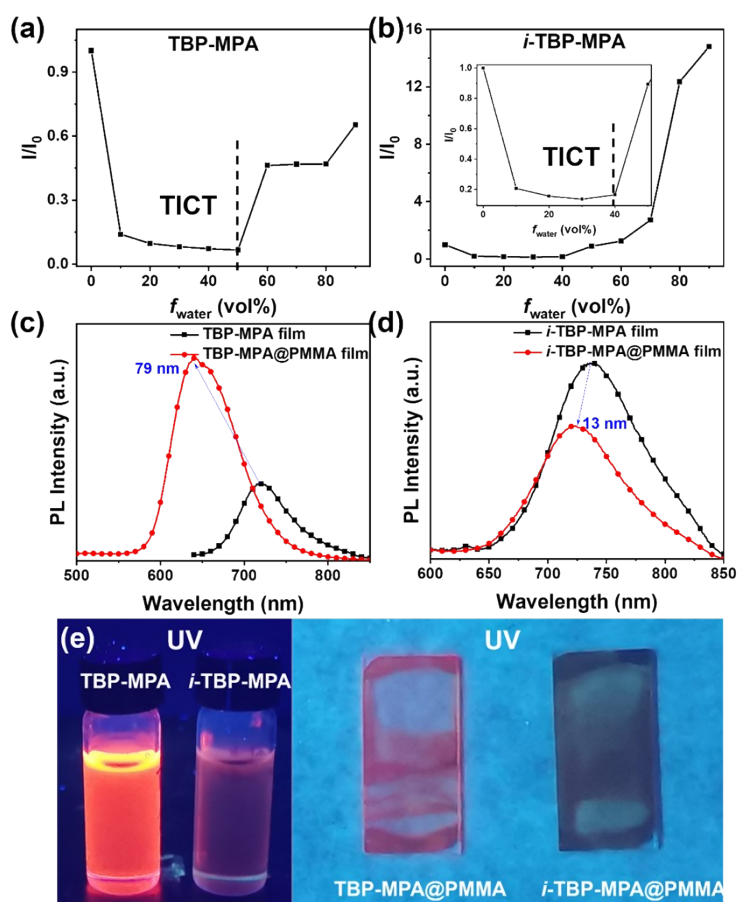

Figure S7. Maximum emission intensity plots of (a) TBP-MPA and (b) *i*-TBP-MPA in THF/H$_2$O mixtures. Inset: Decrease in fluorescence intensity influenced by TICT effect. PL spectra of (c) TBP-MPA and (d) *i*-TBP-MPA in pure and doped films. (e) Photographs of TBP-MPA and *i*-TBP-MPA in toluene solutions and doped PMMA films under UV irradiation.
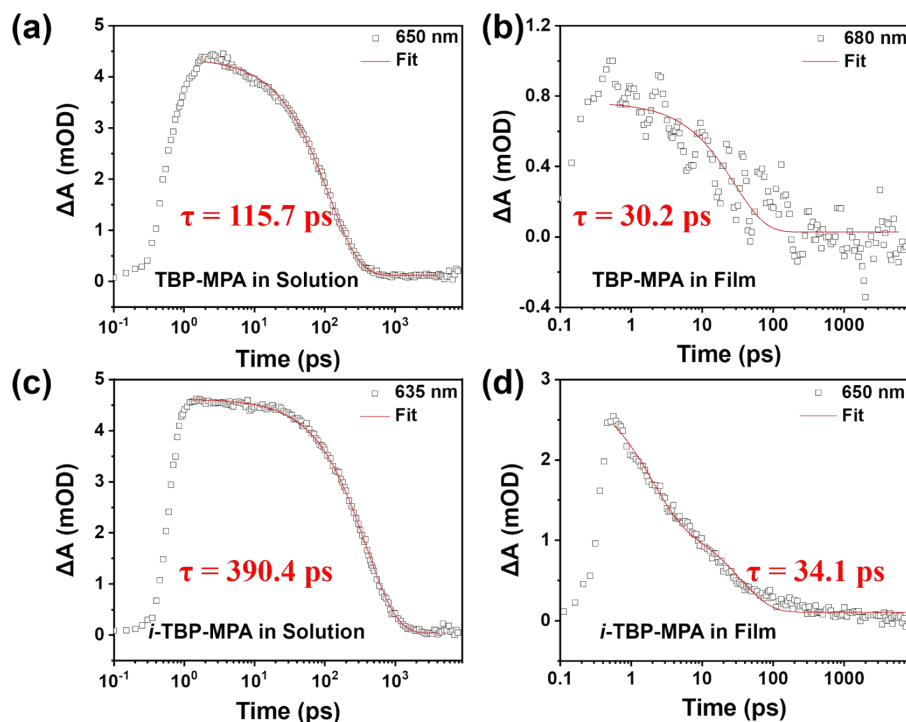
Figure S8. (a) Overlap diagram of optimized S_0 (blue) and S_1 (red) geometries of TBP-MPA. (b) The atomic arrangement in the TBP-MPA molecule. (c) The contributions of different parts of the TBP-MPA molecule to the recombination energy. (d) Calculated Huang-Rhy factors of TBP-MPA.

Figure S9. (a) Overlap diagram of optimized S_0 (blue) and S_1 (red) geometries of *i*-TBP-MPA. (b) The atomic arrangement in the *i*-TBP-MPA molecule. (c) The contributions of different parts of the *i*-TBP-MPA molecule to the recombination energy. (d) Calculated Huang-Rhys factor of *i*-TBP-MPA.

6

Figure S10. (a) TA traces of ESA signals probed at 650 nm recorded from the TBP-MPA solution. (b) TA traces of ESA signals probed at 680 nm recorded from the TBP-MPA film. (c) TA traces of ESA signals probed at 635 nm recorded from the *i*-TBP-MPA solution. (d) TA traces of ESA signals probed at 650 nm recorded from the *i*-TBP-MPA film.

Table S1. Calculated excited wavelength and oscillator strengths and related wave functions.

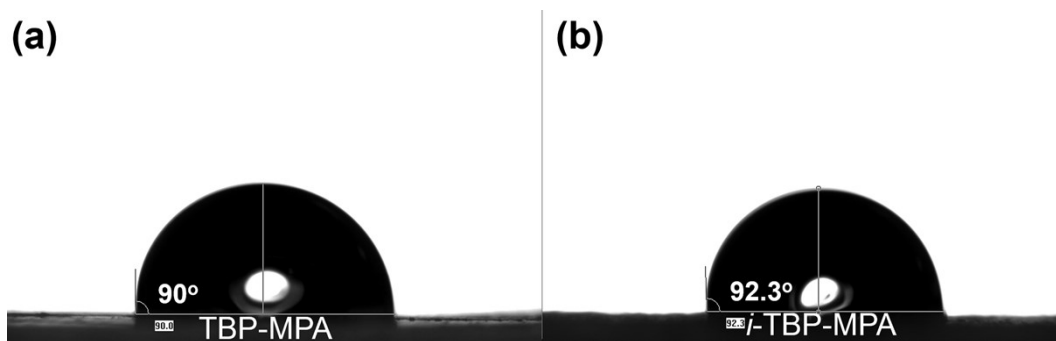| Electronic transition		Excitation energies (eV)	λ (nm)	oscillator strength	Configuration	
TBP-MPA	$S_0 \rightarrow S_1$	1.7617	703.76	0.1263	HOMO→LUMO	98.9%
	$S_0 \rightarrow S_2$	1.8222	680.43	0.3491	HOMO-1→LUMO	99.4%
	$S_1 \rightarrow S_0$	1.4272	868.72	0.2029	HOMO→LUMO	98.8%
i-TBP-MPA	$S_0 \rightarrow S_1$	1.5920	778.79	0.1930	HOMO→LUMO	98.6%
	$S_0 \rightarrow S_4$	2.6978	459.57	1.0551	HOMO-3→LUMO	29.9%
					HOMO→LUMO+1	67.6%
	$S_1 \rightarrow S_0$	1.2386	1001	0.2257	HOMO→LUMO	98.9%

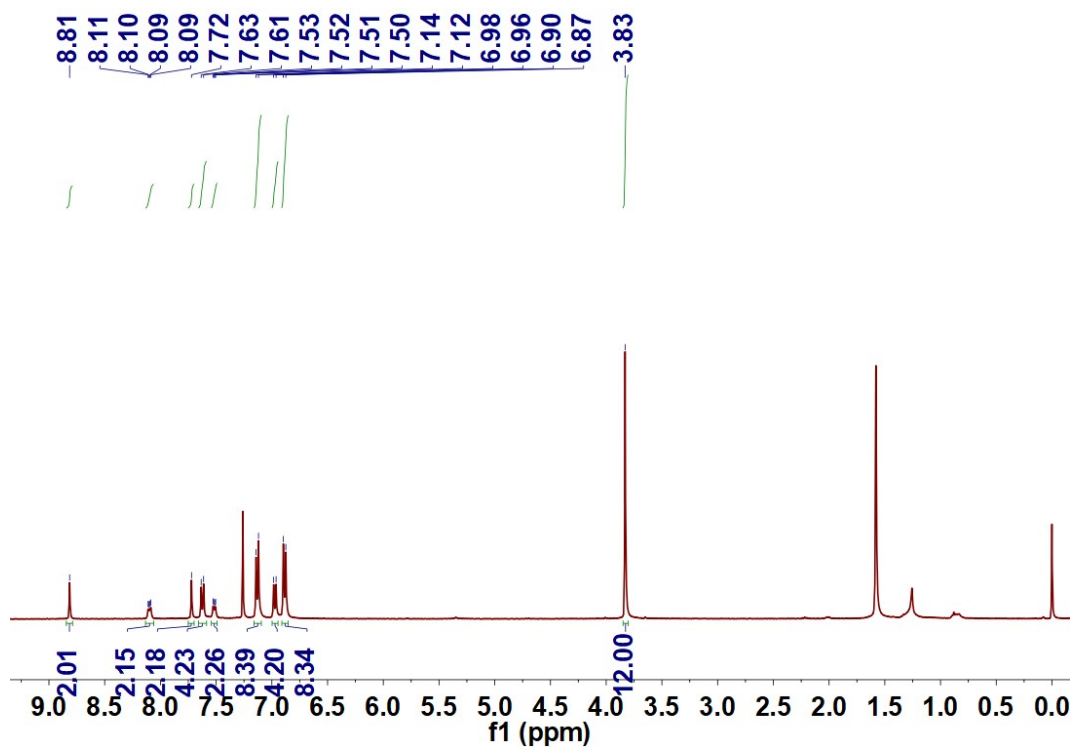**Figure S11.** Water contact angles of (a) TBP-MPA and (b) *i*-TBP-MPA.

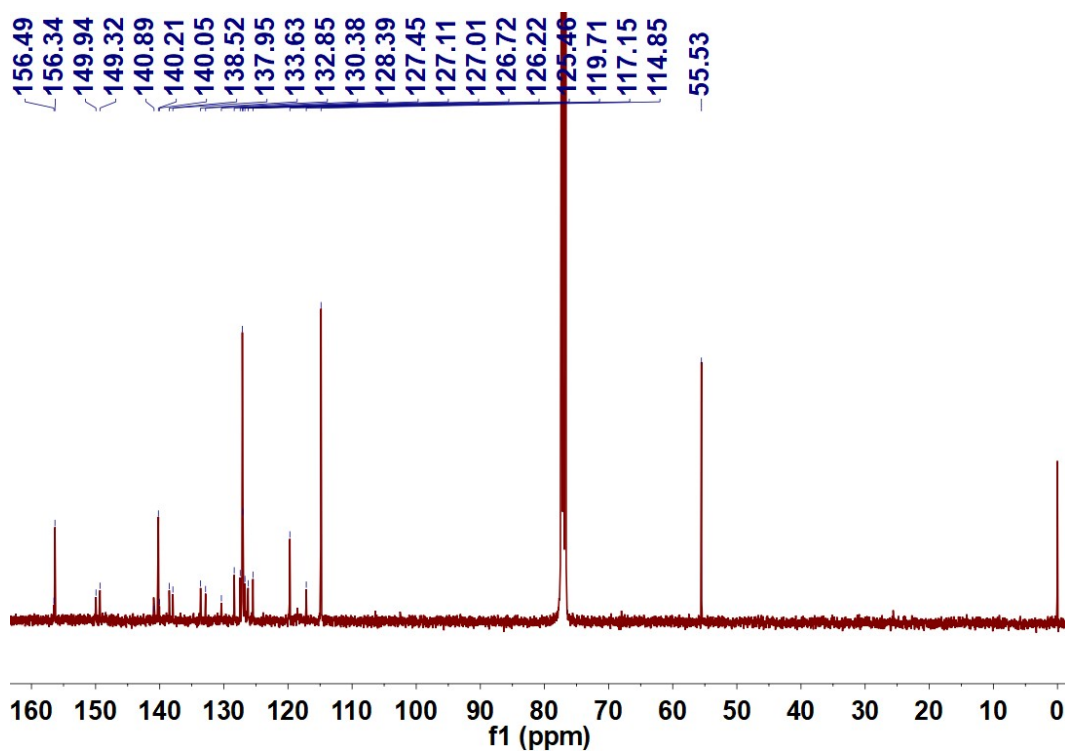**Figure S12.** ¹H-NMR spectrum (400 MHz) of TBP-MPA in CDCl₃.
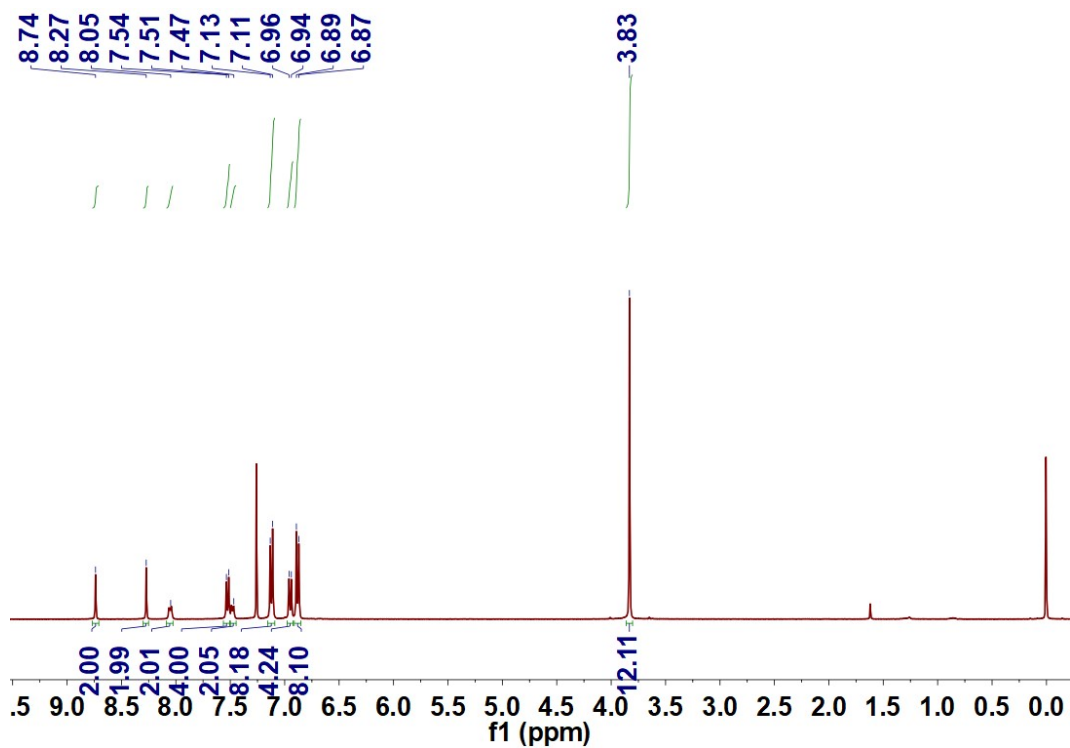
Figure S13. ^{13}C-NMR spectrum (101 MHz) of TBP-MPA in CDCl$_3$.

Figure S14. ^{1}H-NMR spectrum (400 MHz) of *i*-TBP-MPA in CDCl$_3$.
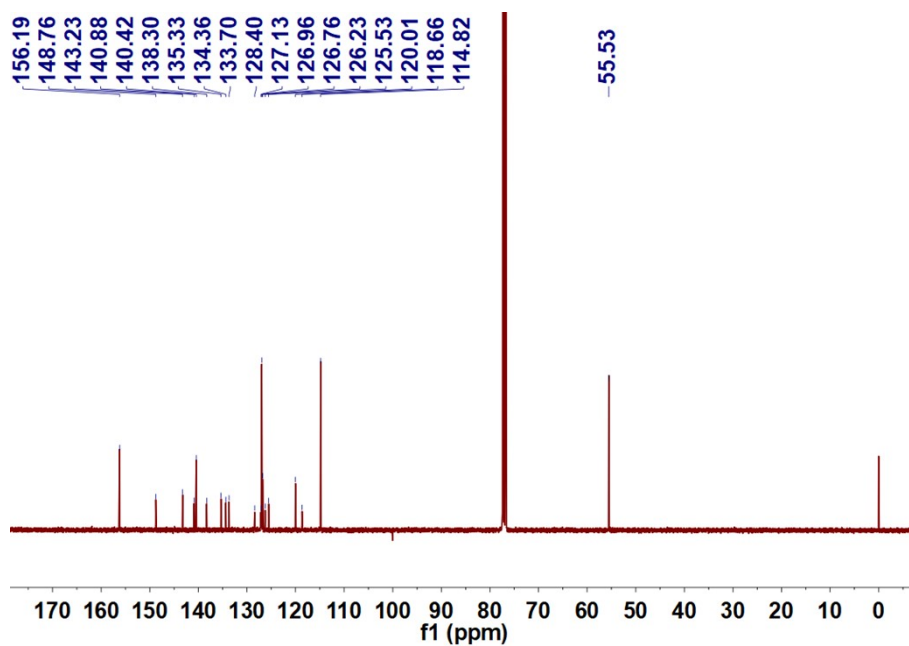
9

Figure S15. ^{13}C-NMR spectrum (101 MHz) of *i*-TBP-MPA in CDCl$_3$.
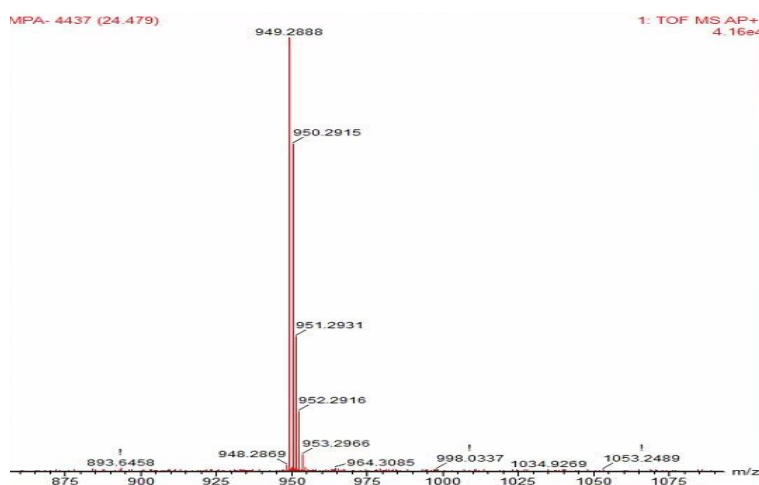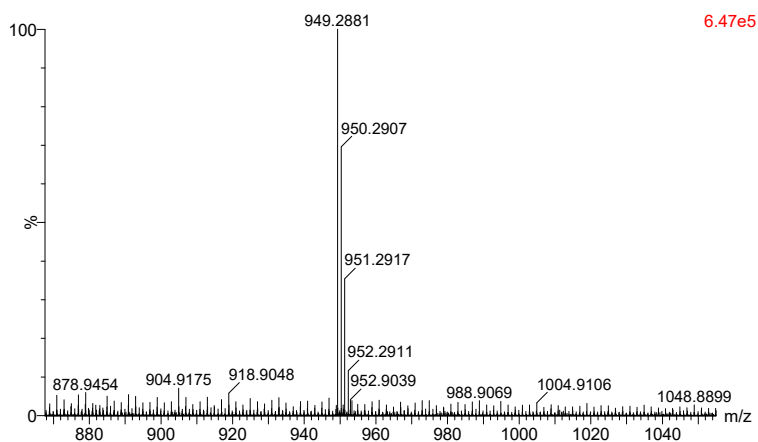

Figure S16. HRMS spectrum of TBP-MPA.

Figure S17. HRMS spectrum of *i*-TBP-MPA.

10

References

[1] L. Chen, B. Zhang, Y. Cheng, Z. Xie, L. Wang, X. Jing, F. Wang, *Adv. Funct. Mater.* **2010**, *20*, 3143-3153.

[2] Y. Li, S. Liu, H. Ni, H. Zhang, H. Zhang, C. Chuah, C. Ma, K. S. Wong, J. W. Y. Lam, R. T. K. Kwok, J. Qian, X. Lu, B. Z. Tang, *Angew. Chem. Int. Ed.* **2020**, *59*, 12822-12826.

[3] a) S. N. Intorp, M. Hodecker, M. Müller, O. Tverskoy, M. Rosenkranz, E. Dmitrieva, A. A. Popov, F. Rominger, J. Freudenberg, A. Dreuw, U. H. F. Bunz, *Angew. Chem. Int. Ed.* **2020**, *59*, 12396-12401; b) A. Meyer, E. Sigmund, F. Luppertz, G. Schnakenburg, I. Gadaczek, T. Bredow, S.-S. Jester, S. Höger, *Beilstein J. Org. Chem.* **2010**, *6*, 1180-1187.

[4] Frisch, M. J.; Trucks, G. W.; Schlegel, H. B.; Scuseria, G. E.; Robb, M. A.; Cheeseman, J. R.; Scalmani, G.; Barone, V.; Petersson, G. A.; Nakatsuji, H. et al. Gaussian 16, Gaussian, Inc.: Wallingford, CT, **2016**.